THE EFFECT OF SERVICE EXPOSURE ON THE CREEP PROPERTIES OF CAST IN-738LC SUBJECTED TO LOW STRESS HIGH TEMPERATURE CREEP CONDITIONS

R. Castillo,* A.K. Koul** and J-P.A. Immarigeon**

*Product Reliability Department
Turbine and Generator Division
Westinghouse Canada Inc.
Hamilton, Ontario, Canada

**Structures and Materials Laboratory
National Aeronautical Establishment
National Research Council of Canada
Ottawa, Ontario, Canada

SUMMARY

Constant load (90 MPa) creep properties of specimens machined from new and service exposed IN-738LC turbine blades are reported for testing temperatures in the range of 899 to 996°C. The rupture lives in these tests varied between 250 to 10,000 hours.

There appears to be a transition temperature ($\sim$ 960°C) above and below which intragranular and grain boundary sliding deformation mechanisms predominate in IN-738LC at 90 MPa. Under intragranular deformation conditions, service exposed blades exhibit an increase in $\dot{\epsilon}_m$ and ϵ_r relative to new blades because the coarse γ' precipitates in service exposed blades facilitate flow. Under grain boundary sliding deformation conditions, however, the service exposed blades exhibit a decrease in $\dot{\epsilon}_m$ and ϵ_r relative to new blades because service induced break down of MC carbides produces continuous networks of grain boundary $M_{23}C_6$ carbides which suppress the sliding more effectively during creep testing.

The rupture life in both new and service exposed blades appears to be governed by stress assisted environmental cracking rather than any deformation mechanisms 'per se.' Fracture in both materials occurs through the link-up of environmentally induced surface cracks with the creep induced internal cracks. Final fracture occurs by transgranular shear. The service exposed blades contain slightly lower Cr content in the grain boundary regions because of heavy $M_{23}C_6$ precipitation along the grain boundaries. It is suggested that the reduced oxidation resistance of the grain boundary regions in service exposed blades increases the severity of oxidation and results in marginally lower rupture lives during creep testing.

Superalloys 1988
Edited by S. Reichman, D.N. Duhl,
G. Maurer, S. Antolovich and C. Lund
The Metallurgical Society, 1988

Introduction

The effects of extended service times upon the mechanical properties of cast nickel base superalloy components in hot sections of gas turbine engines are not well understood. A series of time and stress dependent solid state precipitation reactions occur at service temperatures in these components that can adversely affect their structural integrity.[1]

Accelerated creep testing has generally been employed to demonstrate the effects of service exposure on mechanical properties, usually by conducting tests at stresses and temperatures higher than those experienced during service. The problem with this approach is that the deformation and fracture mechanisms during testing may be quite different from those prevailing under service conditions. In particular, the fracture mode can change from transgranular to intergranular as the deformation temperature is increased.[2] Such transition has also been observed in IN-738LC at constant creep testing temperature with changes in grain boundary microstructure.[3] Therefore, in order to analyze the effects of service-exposure on the mechanical properties of hot parts, it is important to understand the microstructure property relationships during creep testing at near service stresses and temperatures.

This paper reports the results of a study on the relationship between microstructure and creep behaviour of conventionally cast IN 738LC, a nickel base superalloy, tested at a low stress and high temperatures representative of approximate service conditions. The main purpose of the study was to provide information leading to the identification of the failure mechanism, which is the subject of some controversy for alloys of this type.[4] The investigation involved an evaluation of the microstructural changes caused by service and their influence on post-exposure properties when compared to the material in the unexposed condition.

Experimental Procedure

The material selected for the study was obtained as precision cast turbine blades with nominal compositions as shown in Table I. Creep data were generated for one new blade and two used blades which had been in service for 14,000 and 31,000 hours respectively. The blade temperature in mid-airfoil section during service is known to be in the range of 830°C to 845°C.[3,5]

All as-cast blades had been hot isostatically pressed (HIPed) at 1200°C/2 hours, ramp-cooled to 1120°C and then furnace cooled to room temperature. Post-HIP heat treatments included solutioning at 1120°C/2 hours followed by an air cool and aging at 845°C/24 hours followed by air cooling to room temperature. Microstructures of blades were evaluated by optical and scanning electron microscopy. The details of this evaluation are reported elsewhere.[3,5] Creep tests were conducted in air, on

TABLE I

NOMINAL COMPOSITION IN WEIGHT % OF COMMERCIAL CAST IN-738 LC ALLOY

Material Condition	C	Mo	Cr	Ni	W	Fe	Co	Al	Ti	Nb	Ta	Zr	B	Mn	Si	P	Cu
Unexposed	.10	1.74	16.01	Bal.	2.66	.12	8.35	3.44	3.40	.81	1.66	.03	.01	<.10	<.10	<.10	<.10
14,000 hr Service	.09	1.77	16.03	Bal.	2.51	.12	8.36	3.44	3.49	.83	1.66	.03	.01	<.10	.03	.005	<.05
31,000 hr Service	.09	1.70	15.9	Bal.	2.59	.10	8.29	3.37	3.36	.70	1.64	.04	.01	<.10	<.10	.004	<.10

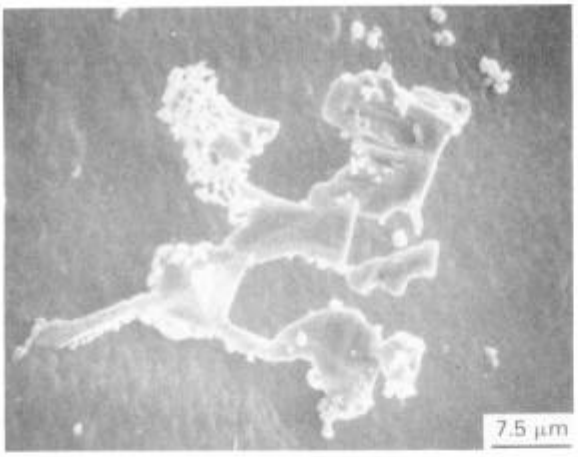

Fig. 1. Intragranular MC carbide and $M_{23}C_6$ carbides attached to its surface as a result of its decomposition.

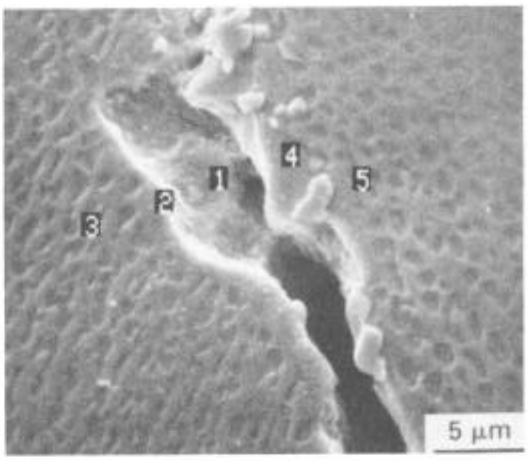

Fig. 2. Fractured grain boundary area of a crept specimen. The Cr Concentration in spot nos. 1 = 9.63%, 2 = 14.86%, 3 = 15.12%, 4 = 7.83% and 5 = 15.96% in wt. %.

specimens machined from mid-airfoil sections of blades, in constant load creep machines at 90 MPa and at temperatures between 899 and 996°C. The creep specimens had a gage diameter of 4.0 mm and a gage length of 19.0 mm. Creep strain was measured with an accuracy of greater than ± 0.01 pct by means of a linear variable displacement transducer (LVDT).

Results

Previous studies have indicated that γ' precipitates coarsen and MC carbides degenerate in these blades during service.(3,5) Primary MC carbides break down into $M_{23}C_6$ carbides which precipitate preferentially along grain boundaries, thus modifying the original grain boundary microstructure. Evidence of MC carbide degeneration is shown in Fig. 1. Free carbon released by MC carbide decomposition diffuses rapidly to the grain boundaries, reacting with surrounding Cr to form $M_{23}C_6$ carbides, with the result that the grain boundary regions are depleted in Cr, Fig. 2. Since Cr is the key element responsible for the corrosion resistance of the alloy, the reduction in Cr content close to the grain boundaries increases the susceptibility of the material to intergranular oxidation.

In both new and service exposed materials, several types of MC carbides were detected that were rich in the usual carbide forming elements, namely, Ti, Nb and Ta. Approximate compositions of the four types of MC carbides that were identified are given in Table II.

TABLE II

METALLIC ELEMENT COMPOSITION (in wt. pct.) OF INTRAGRANULAR MC CARBIDES

	Ta	Nb	Ti	Cr	Co	Ni
MC_I	47.0	19.0	30.0	1.4	1.6	3.0
MC_{II}	28.0	31.0	30.0	2.0	1.3	7.9
MC_{III}	15.0	6.5	75.0	1.2		2.0
MC_{IV}	26.0	11.0	58.0	1.6		3.0

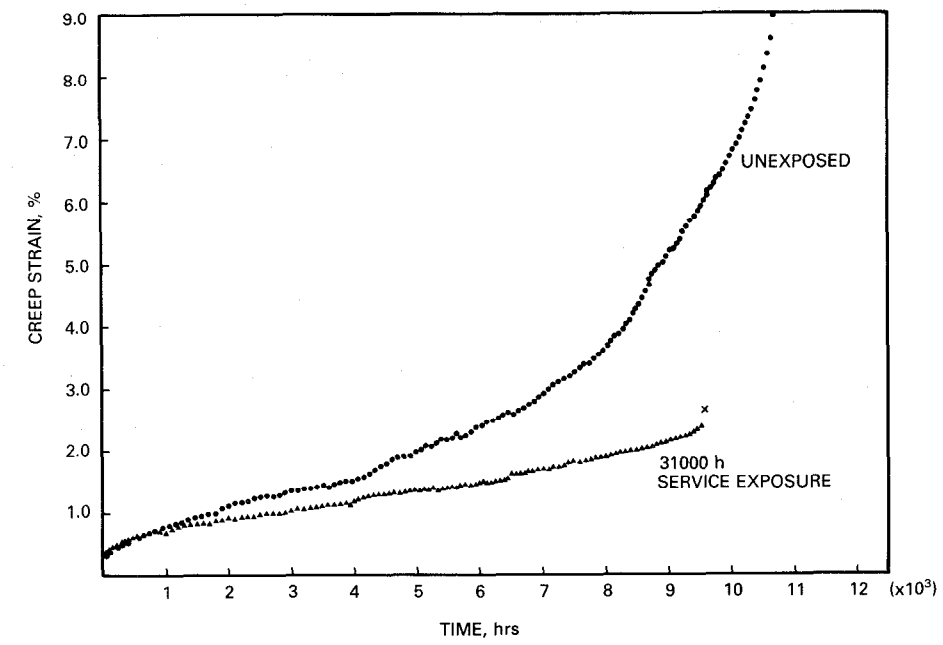

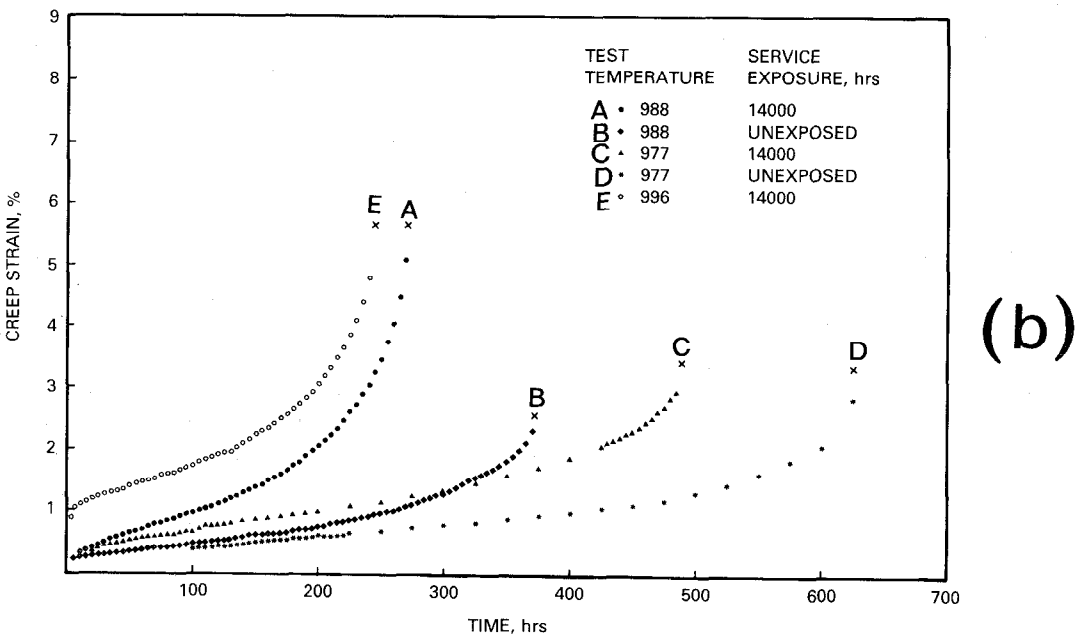

Fig. 3 Effect of service exposure on the creep behaviour of new and service exposed IN-738LC blades tested at 90 MPa and (a) 899°C and (b) 977, 988 and 996°C.

Creep testing Results

Creep curves for long term (low temperature) and short term (high temperature) testing conditions are shown in Figs. 3a and 3b respectively. The data indicate that compared to new blades higher creep rates prevail during short term tests in service-exposed material whereas the reverse is observed during long term tests of the order of 2,000 to 10,000 hours.

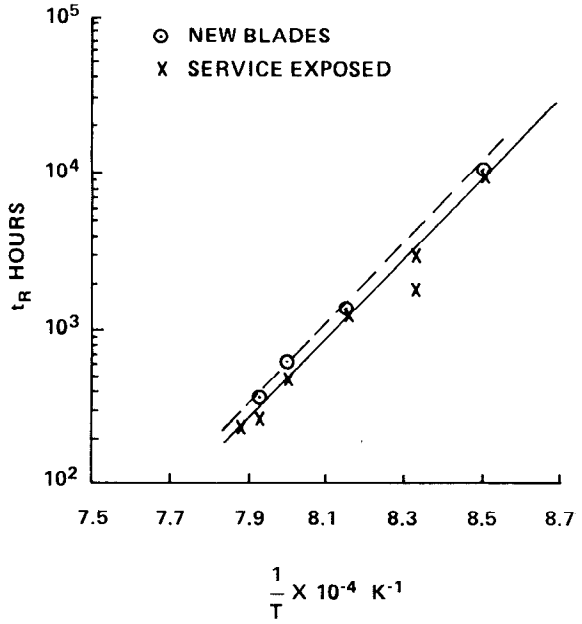

Fig. 4 Effect of creep testing temperature on t_r of new and service exposed blades at 90 MPa.

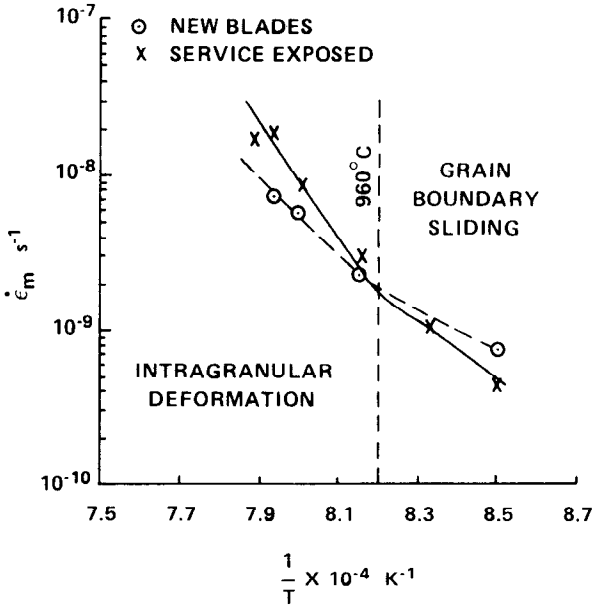

Fig. 5 Effect of creep testing temperature on $\dot{\epsilon}_m$ of new and service exposed blades at 90 MPa.

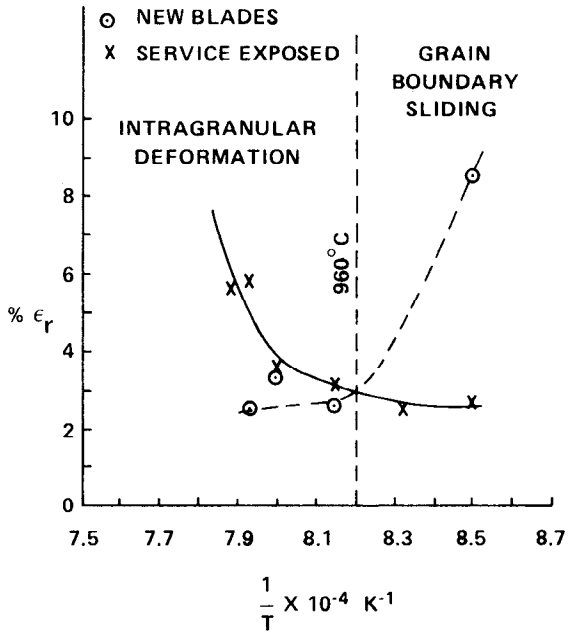

Fig. 6 Effect of creep testing temperature on ϵ_r of new and service exposed blades at 90 MPa.

The effects of service-exposure on rupture life, t_r, minimum creep rate, $\dot{\epsilon}_m$, and creep ductility, ϵ_r, for all test conditions examined can be seen in Figures 4, 5 and 6, respectively. Under comparable testing conditions, the service-exposed material exhibited rupture lives that were marginally lower than those for the new material, Figure 4. However, there were noticeable differences in $\dot{\epsilon}_m$ and ϵ_r that varied in magnitude with test temperature. Below approximately 960°C, the service-exposed material exhibited lower $\dot{\epsilon}_m$ values whereas above this temperature, its $\dot{\epsilon}_m$ was higher, Fig. 5. Similarly, compared to new blades ϵ_r for service exposed

material was lower below 960°C and higher above this temperature, Fig. 6. It thus appears that 960°C is a transition temperature above and below which different deformation mechanisms operate leading to differences in $\dot{\epsilon}_m$ and ϵ_r between the new and service-exposed material.

Microstructures of Crept Specimens

There was evidence of enhanced γ' coarsening and rafting near the grain boundaries in specimens tested at lower temperatures in long term tests, Fig. 7. This indicates that flow localization occurs in regions adjacent to the grain boundaries and may be viewed as an accommodation to grain boundary sliding. There was also some evidence of γ' rafting in short term tests at high test temperatures, Fig. 8, although the γ' coarsening was minimal in this case. These observations suggest that grain boundary sliding predominates at lower test temperatures whereas intragranular deformation predominates at higher test temperatures below and above the 960°C transition, Figs. 5 and 6.

After creep testing at lower temperatures, under near service conditions, iron rich areas were observed along the grain boundaries of the new material Fig. 9. It is not clear what role these Fe-rich areas play in the creep behaviour of Ni-base superalloys.

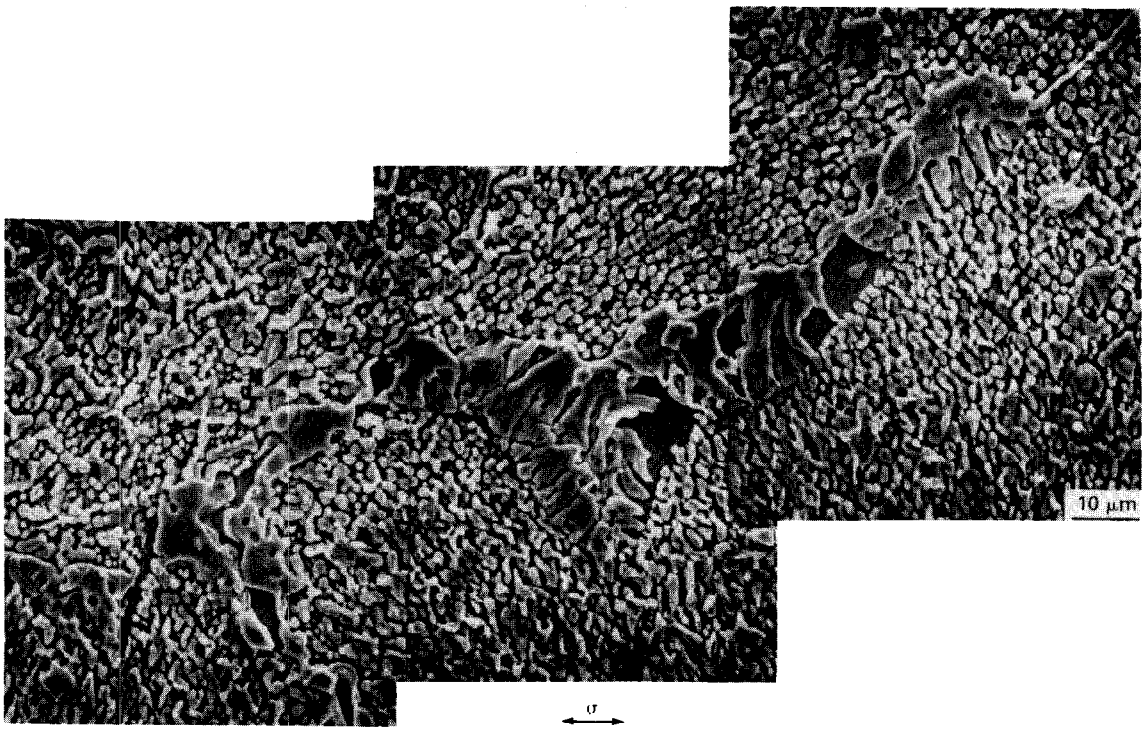

Fig. 7 Typical grain boundary structure of the new blade specimen creep tested at a lower temperature (899°C) at 90 MPa showing grain boundary γ' coarsening and rafting .

Fracture Behaviour of Crept Specimens

All specimens tested to rupture contained cavities and cracks at grain boundaries and oxidized surface cracks at intergranular sites, Fig. 10. In all cases, surface grain boundary cracks were larger than internal cracks and were mostly normal to the tensile stress axis. Intragranular /interdendritic fracture features were observed in both new and service exposed materials up to approximately one-half of the specimen gage section, Fig. 10. The fast fracture areas showed the appearance of typical transgranular shear inclined at about 45° to the specimen axis, Fig. 10.

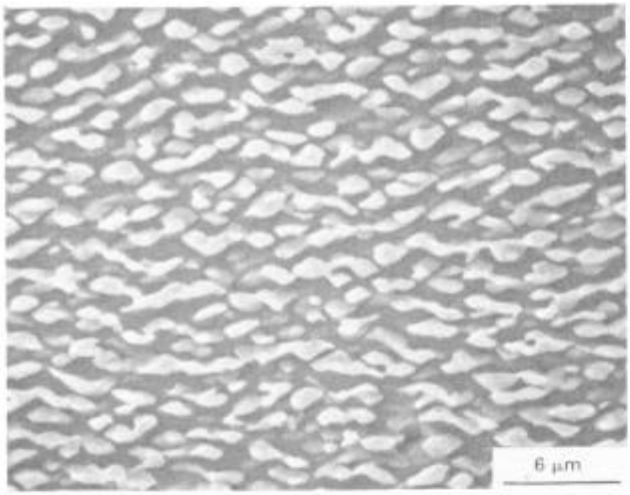

Fig. 8 Some γ' rafting in new blade specimen creep tested at 977°C and 90 MPa.

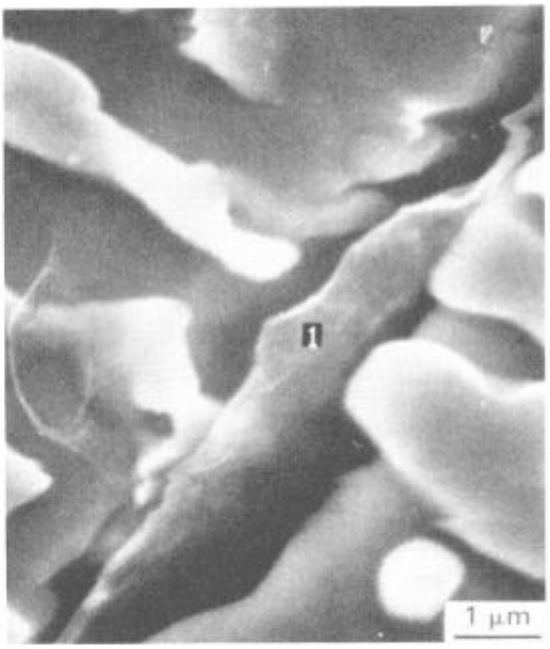

Fig. 9 Example of an Fe rich region in a new blade sample creep tested at 899°C and 90 MPa. In spot No. 1 Fe = 4.18 wt.% and in the matrix Fe = 0.12 wt.%.

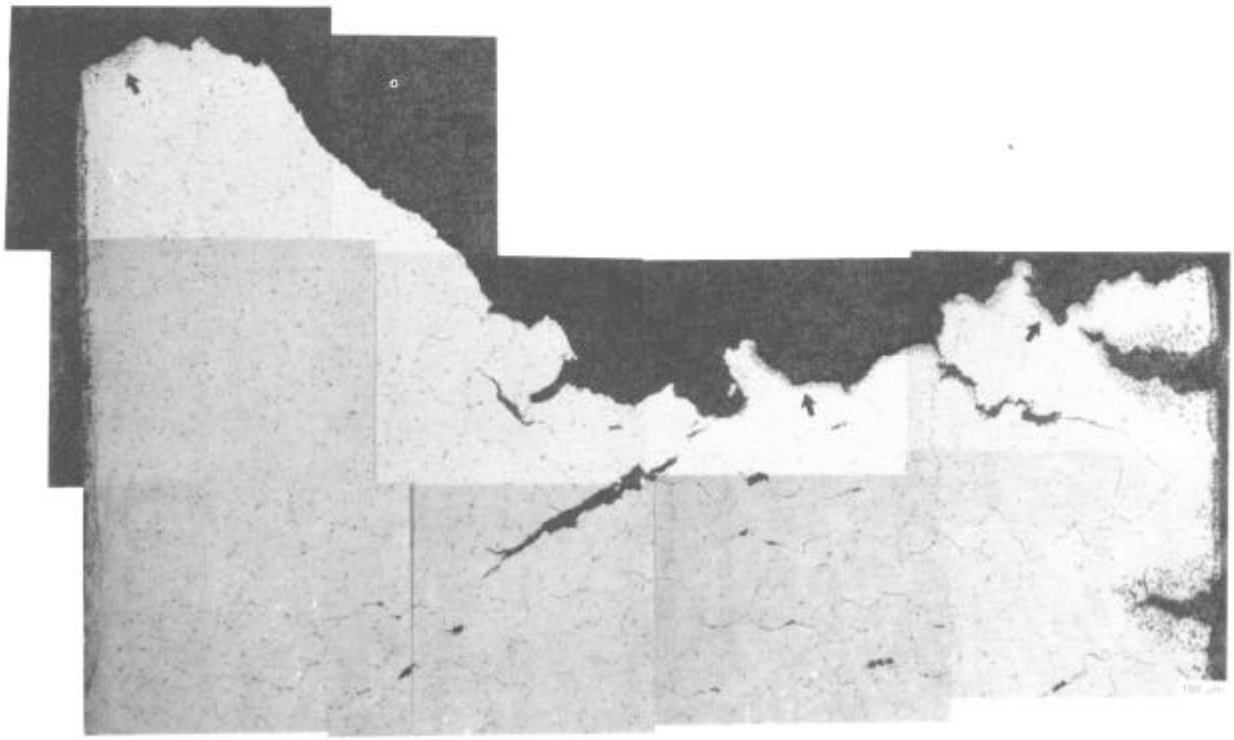

Fig. 10 Optical micrograph showing evidence of intergranular oxide penetration (arrows), micro-cracking and transgranular shear.

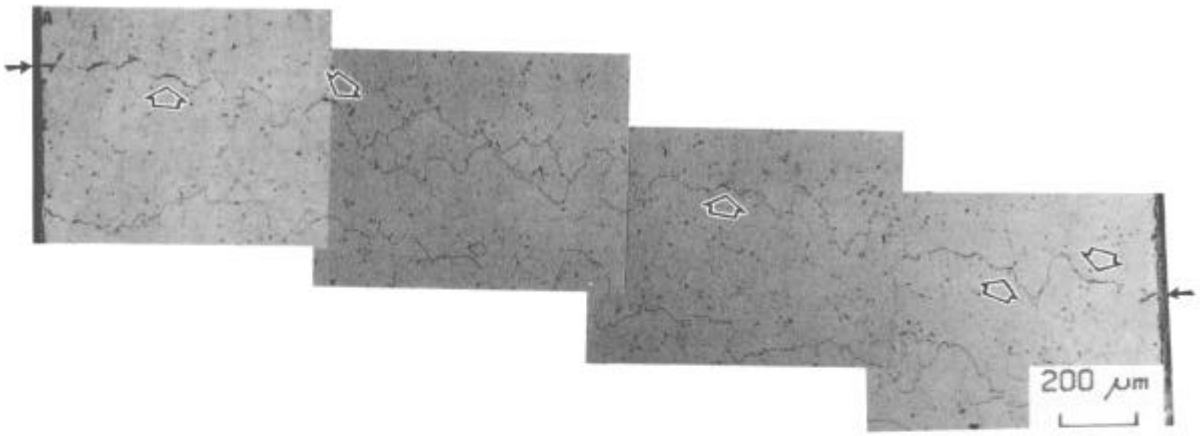

Fig. 11 Grain boundary surface cracks (arrows) and early stages of internal crack link-up (open arrows) in a service exposed specimen creep tested at 927°C and interrupted during early stages of secondary creep.

Damage in the gage length of the crept specimens showed important differences between the new and service exposed specimens that were creep tested at temperatures below 960°C. The 899°C creep tests indicated that the new material contained relatively more creep cavities than the service exposed material under identical creep loading conditions. Internal cracking was also more extensive in the new material than the service exposed material. These observations suggest that below 960°C the continuous networks of grain boundary $M_{23}C_6$ carbides in the service exposed material suppress deformation in the grain boundary regions. At creep testing temperatures above 960°C, however, the differences in the fracture behaviour of the new and service exposed specimens were less obvious.

Interrupted creep tests indicated that environmentally assisted intergranular cracking occurs early during secondary creep in both new and service exposed materials, Fig. 11, and concurrently the internal grain boundary cracking also occurs within the bulk of the material. Final fracture appears to take place through the link up of the surface crack with the internal cracks in all cases, Figs. 10 and 11.

Discussion

The results indicate that there is a transition in the predominant deformation mechanism as the creep testing temperature decreases. At 90 MPa, the transition occurs around 960°C in the alloy investigated, Figs. 5 and 6. The activation energies (Q) for the deformation processes, below and above the transition temperature, were calculated based on power law fits through the data of the form:

$$\dot{\epsilon}_m = A\, e^{-Q/RT} \sigma^n \qquad \ldots\ldots\ldots\ldots\ldots\ldots\ldots\ldots (1)$$

where σ is the applied stress, Q is the activation energy, T is the test temperature, R is the gas constant and A and n are material constants. Below 960°C the Q values were of the order of 16-22 KCal/mole whereas above the transition temperature they were approximately 30-40 KCal/mole for both new and service exposed materials. While the Q values below and above the transition temperature do not match the activation energy values for grain boundary or volume diffusion of various alloying additions in Ni, it is significant that below 960°C the Q values are roughly one half the value observed above 960°C. The deviation in the actual magnitude of Q from that reported for intragranular and grain boundary sliding deformation mechanisms is not totally unexpected. The true Q values for a given deformation mechanism can only be obtained providing the structure is kept

constant, a condition that cannot be satisfied in metastable Ni-base alloy systems. However, in view of the evidence for flow localization adjacent to the grain boundaries, (Fig. 7), the crossover in $\dot{\epsilon}_m$, (Fig. 5) and the smaller Q values below the transition temperature it can be argued that grain boundary sliding predominates below 960°C whereas intragranular flow predominates above 960°C.

The differences in the overall creep behaviour of new and service exposed blades can be rationalized in terms of the differences in the intragranular and grain boundary microstructural features of the two materials. Above 960°C, the intragranular deformation mechanism predominates and the service exposed blades are expected to show an increase in $\dot{\epsilon}_m$, and ϵ_r, Figs. 5 and 6, because they contain coarse γ' precipitates which lower the grain strength . In contrast, below 960°C, the grain boundary sliding mechanism predominates and the service exposed blades would be expected to show lower $\dot{\epsilon}_m$ and ϵ_r values, Figs. 5 and 6, because continuous carbide networks in service exposed blades will suppress the grain boundary sliding more effectively.

The similar t_r values of the new and service exposed material at comparable testing temperatures can be attributed to the fact that stress and environment assisted crack nucleation and propagation controls t_r rather than a specific deformation mechanism 'per se'. For both materials final fracture occurs in air as a consequence of the propagation of one or several of the surface initiated cracks nucleated early during the secondary stage of creep. Fig. 10 shows the profile of a crack, which was able to follow the transverse grain boundary to a greater depth causing final fracture. Oxides and nitrides were observed around the crack surface. Similar surface nucleated cracks, located in the specimen shoulder section, showed minimal grain boundary oxidation. Clearly, the rate of oxygen penetration along the grain boundaries is greatly enhanced by applied stress. The manner in which oxygen prompts grain boundary embrittlement leading to intergranular failures could be explained by a mechanism originally proposed by Briknell and Woodford.(6) Initially, the boundary is embrittled by oxygen penetration in the near surface region. This embrittled boundary fails afterwards in tension and the free surfaces thus produced are oxidized while oxygen diffuses down the boundary ahead of the crack. It appears that oxygen penetration along grain boundaries indeed precedes actual crack formation. The metallographic evidence suggests that the extremely low Cr content in the boundary regions plays some role during fracture because of the reduced oxidation resistance of the grain boundaries. The marginally lower t_r values of the service exposed blades are perhaps related to this effect, Fig. 4.

Conclusions

The results demonstrate that short term creep testing does not reveal loss of creep ductility due to grain boundary embrittlement in service exposed blades. This is because intragranular deformation mechanisms are dominant during short term testing whereas grain boundary sliding predominates under service conditions.

References

1. J.W. Martin and R.D. Doherty, "Stability of Microstructure in Metallic Systems," (University Press: Cambridge, 1976).

2. H.R. Tipler et. al, Proc. Conf. "High Temperature Alloys for Gas Turbines," Liege, Belgium, September 25-27, 1978, Applied Science Pub., 359-407
3. R. Castillo and A.K. Koul, Proc. Conf. "High Temperature Alloys for Gas Turbines and Other Applications," Liege, Belgium, October 6-9, 1986, p. 1395-1410.
4. S. Ogersby and T.B. Gibbons, "Creep Cavitation in Cast Ni-Cr Base Alloy," J. Mat. Sci and Eng., 59 (1983), L11-L14
5. A.K. Koul and R. Castillo, "Assessment of Microstructural Damage and Its Rejuvenation in Turbine Blades," Met. Trans. A, In Press, 1988.
6. R.H. Briknell and D.A. Woodford, "Grain Boundary Embrittlement of the Fe-Base Superalloy IN-903," Met. Trans A., 12 (1981) 1673-1680.